Engineering and Technology Journal
Journal homepage: https://etj.uotechnology.edu.iq

Experimental Investigation on Heat Transfer in A Gas-Solid Fluidized Bed with A Bundle of Heat Exchanging Tubes

Zahraa W. Hasan[a], Abbas J. Sultan[a,b], Maryam Tariq[a], Laith S. Sabri[a,b], Hussein G. Salih[a], Jamal M. Ali[a]*, Muthanna H. Al- Dahhan[b]

[a]Chemical Engineering Dept., University of Technology-Iraq, Alsina'a street,10066 Baghdad, Iraq.
[b]Department of Chemical and Biochemical Engineering, Missouri University of Science and Technology (MS&T), Rolla, MO.
*Corresponding Author Email: jamal.m.ali@uotechnology.edu.iq

HIGHLIGHTS

- An experimental investigation was carried out in mimicked Fischer-Tropsch fluidized bed reactor with vertical heat exchanging tubes.
- An advanced heat transfer technique was used to quantify the heat transfer coefficient locally and instantaneously.
- The impact of vertical heat exchanging tubes on the local heat transfer coefficient was investigated.
- The findings of this study would further improve the knowledge of the impact of vertical heat exchanging tubes on heat transfer in gas-solid fluidized bed reactor.

ARTICLE INFO

Handling editor: Saad. Al-Saadi

Keywords:
Fluidized bed reactor; Vertical heat exchanging tubes; Local heat transfer coefficient; Advanced heat transfer technique; Silica sand particle.

ABSTRACT

A fluidized bed reactor is commonly used for highly exothermic reactions for different chemical industrial processes. However, inefficient removal of the generated heat due to the exothermic reaction can seriously influence reactor performance. Hence, quantifying and understanding the heat transfer phenomena in this reactor is essential to enhance the performance of the reactor and, consequently, the chemical process. To achieve a better quantification and understanding of the heat transfer in this reactor, an advanced heat transfer technique has been used in this study to quantify the impact of the presence of the cooling tubes on the local heat transfer coefficient at four radial positions (r/R = +/- 0.58, +/- 0.03) at an axial height of H/D =15 cm from the distributor plate with a wide range of superficial gas velocities (0.2-0.48). It has been found that the local heat transfer coefficient in the fluidized bed reactor equipped with a bundle of vertical tubes increases significantly as superficial gas velocity increases at the wall region, while different behavior was noticed at the center of the reactor. Moreover, the results show that the local heat transfer significantly decreases at the reactor's core region for all studied superficial gas velocities. Furthermore, the new tube arrangement offers a uniform local heat transfer profile for all studied operating conditions. The obtained new high-quality experimental data for the local heat transfer coefficient in a fluidized bed reactor equipped with a bundle of tubes can be used for validation CFD simulations, developing mathematical models, facilitating design, scale-up, and operation of this reactor.

1. Introduction

The depletion of natural energy resources is a serious issue that potentially has catastrophic effects on the world. For example, the utilization of fossil fuels results in the emission of greenhouse gases during power generation, which is responsible for global warming and climate change. Additionally, many non-renewable sources of energy that are utilized by human beings will run out over time. It is difficult to ignore that the power generated from such sources harms the environment and causes serious health problems. Therefore, studies must pay more attention to alternative energy sources to overcome such concerns.

In the last decade, Fischer-Tropsch synthesis (FTS) has received more attention as an alternative source for the production of ultra-clean transportation fuels, chemicals, and other hydrocarbon products through catalytic conversion of the synthesis gas or syngas (i.e., a mixture of H_2 and CO) derived from coal, natural gas, or biomass [1–6].

Moreover, the conversion of syngas can be done with a highly exothermic reaction, as the heat recovery is one of the essential aspects of developing and implementing a reactor system for FTS reactions according to the following reaction equation:

http://doi.org/10.30684/etj.v40i9.1094
Received 8 November 2021; Accepted 25 January 2022; Available online 21June 2022
2412-0758/©Publishing rights belongs to University of Technology's Press, Baghdad, Iraq

This reaction is carried out in five major multiphase reactors: multi-tubular fixed-bed reactor, slurry phase reactor, circulating fluidized-bed reactor, fluidized-bed reactor, and micro-channel or micro-structured reactors [7–12]. However, the fluidized bed reactor is the preferable reactor in FTS when compared to other multiphase reactors because this reactor has an extensive range of applications in a vast array of processes, such as polymerization, FTS, fluid catalytic cracking (FCC), drying, cooling, and solids coating [8,12–17]. The heat generated from the exothermicity of reaction in this reactor is considered one of the main parameters affecting this reactor's performance. Accordingly, inserting a bundle of cooling tubes in this reactor is necessary to eliminate the excessive heat and preserve the reaction temperature for processes with high exothermic reactions. Despite the benefits of using these cooling tubes in removing the excess heat generating, these tubes will affect the hydrodynamics, heat, and mass transfer rates in a very complex way. Quantifying the impact of vertical cooling tubes on hydrodynamics, heat, and mass transfer rates is still poorly understood [12,15,19–21].

Quantifying the influence of vertical cooling tubes' presence on hydrodynamics, heat, and mass transfer rates is needed for efficient design, scale-up, and operation of the fluidized bed reactor for the Fischer Tropsch process. This type of data is highly needed in the literature because the design and scale-up of these reactors equipped with a bundle of cooling tubes are still based on employing the correlations obtained from experimental data collected in fluidized bed reactors without vertical cooling tubes [14, 18, 22–24]. In addition, significant literature contributions have reported on heat transfer in fluidized bed reactors [23–26].

However, these literature contributions mainly focus on quantifying heat transfer in fluidized bed reactors without vertical tubes. Comprehensive investigations of heat transfer in a fluidized bed reactor equipped with a vertical tube bundle are rare.

Still, very few studies investigated the hydrodynamic and heat transfer in gas-solid fluidized bed reactor with different heat exchanging tubes using only one tube inserted horizontally or vertically with silica sand particle [16, 27–31].

Therefore, this study aims to investigate for the first time the impact of a bundle of vertical heat exchanging tubes on the instantaneous and local heat transfer coefficient in a mimicked FTS fluidized bed reactor operating under different operating conditions with a square-pitch tubes arrangement using an advanced heat transfer technique. Also, the experiments were carried out using sand particles with a uniform particle size of 600µm

The obtained results and findings will improve the fundamental understanding of the impact of a bundle of tubes on local heat transfer in fluidized bed reactors. Moreover, the collected experimental data will serve as benchmarking data for validating simulations and mathematical models. Furthermore, the gathered experimental data guide designing, scaling up, and operating fluidized bed reactor for Fischer Tropsch synthesis.

2. Material and Methods

2.1 Materials

The bed material used in this study was silica sand particles with a uniform particle size of 600 µm that was sieved to a standard size of 600 µm with a bulk density of 1570 kg/m^3. Table (1) exhibits the properties of this type of particle. It is important to highlight that a material's particle size can significantly impact how it performs in applications. Therefore in this study, a sieve analysis technique was performed.

2.2 Experimental Work

2.2.1 Experimental setup

In this study, an experimental mimicked Fischer-Tropsch fluidized bed reactor has been designed and manufactured from Plexiglas with 0.13 m diameter and 1.83 m height, as shown schematically in Figure 1. In contrast, Figure 2 shows a photo of a fluidized bed equipped with a bundle of heat exchanging tubes.

To simulate the industrial fluidized bed reactor used in FTS, a bundle of thirty stainless steel tubes was designed and manufactured in this work to cover 25% of the cross-sectional area of the fluidized bed reactor[18, 32]. The tubes were arranged using a square pitch tube designed by the SOLIDWORK software and printed by a 3D printer. Figure 3 shows the schematic and photo of the square pitch tube arrangement. Finally, the thirty stainless steel tubes bundle was inserted vertically inside the studied fluidized bed reactor.

Filtered and dried air passed to the column through the plenum section by a gas distributor. This gas distributor is located at the top of the plenum section and is made of porous polyethylene with a pore size and plate thickness of 50 microns and 12.7 mm, respectively. The gas distributor was provided by (Genpore, BB2062-50BB-, USA). The selected gas distributor plate provides uniform air distribution and supports the solid particles' weight after passing through calibrated flowmeter. The calibrated flowmeter was chosen to satisfy the industrial flow rates. Also, this work was carried out using silica sand particles to a static height of 35 cm. Experiments were conducted at superficial gas velocities based on the free cross-sectional area, ranging from 0.2 m/s to 0.48 m/s, adjusted via an air flowmeter.

Table 1: The properties of silica sand particle

Properties	Silica Sand
Particle mean diameter (µm)	600
Particle density(kg/m^3)	1570
Minimum fluidization velocity (m/s)	0.116
Dynamic bed height (cm)	35-60

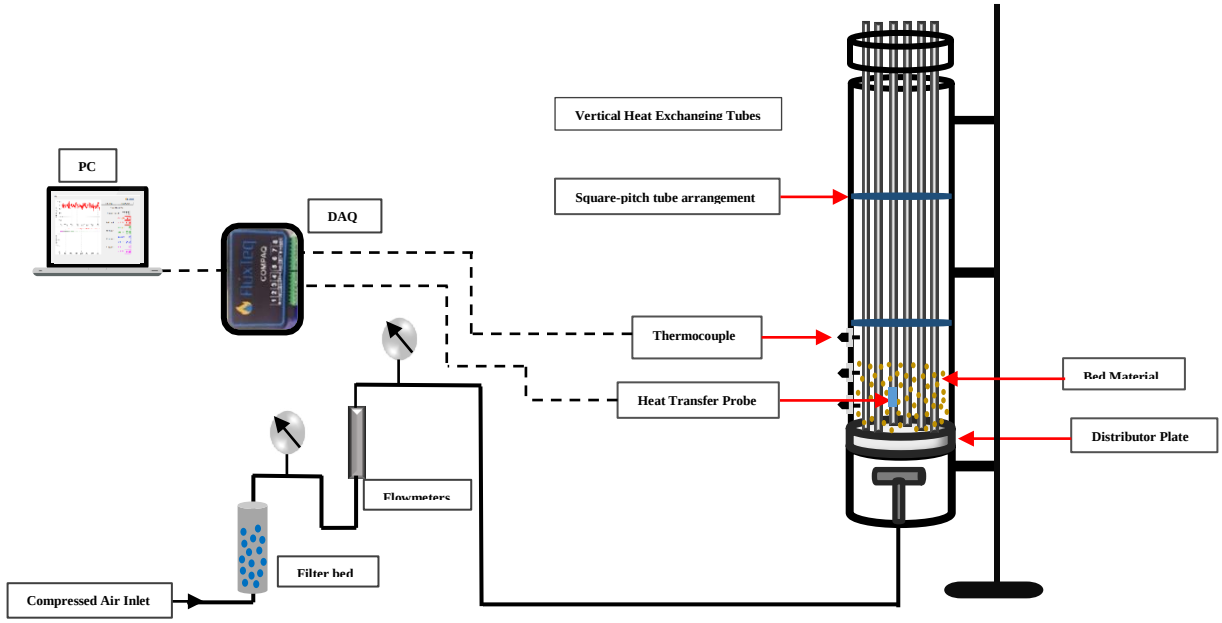

Figure 1: Schematic diagram of gas-solid fluidized bed equipped with vertical heat exchanging tubes

2.2.2 Advanced heat transfer technique

To quantify the impact of vertical heat exchanging tubes in a gas-solid fluidized bed reactor on heat transfer, a fast response heat transfer technique was used to measure the heat transfer coefficient locally and instantaneously.

The advanced heat transfer technique consisted of a heat transfer probe with an inner diameter of 12mm with a length of 8cm, with a piece of solid brass, a heat flux sensor, heater, and two Teflon pieces on both sides of the brass piece to minimize the heat losses within the edges of the probe. The heat transfer probe was fabricated by slicing the brass piece to fit the cartridge heater inside it. Moreover, a cartridge heater (Heatron, Inc. Leavenworth, Kans., USA) was inserted within the space of the brass piece, then the PHFS heat Flux sensor (Flux Teq's LLC, Blacksburg, VA240606370, USA) was flash mounted to the outer surface of a brass piece.

This heat flux sensor was used to measure and quantify the thermal energy per unit area and the surface temperature locally and instantaneously with high sensitivity. Figure 4 and Table 2 display the heat flux sensor photo and schematic diagram with the specifications for this type of sensitive sensor. It is important to mention that a highly stable DC power supply has been used to supply electric power to the heating element with an accurate readout for both voltage and current values.

Three identical thermocouples type T were used to measure the bulk temperature at different positions within a 10 cm distance between each one above the distributor plate. Com PAQ Heat Flux and Thermocouple Data Acquisition Instrument (FluxTeq LLC, Blacksburg, VA240606370, USA) were used to read and record the Flux Teq's PHFS heat flux sensor and integrated temperature sensors with 8 differential channels and handle up to 4 complete PHFS sensors that are measuring both heat flux and temperature. This data acquisition instrument was pre-programmed to accept heat flux leads in channels 1, 3, 5, and 7 and the associated T-type thermocouples in 2, 4, and 6.

Furthermore, this data handles up to 8 channels, the first two channels were used to read out the sensor's heat flux and the surface temperature signals, and the rest were used to quantify the thermocouples signals for each sensor. The program of this data reader provides heat flux and temperature plots for the different channels. Then the data was displayed and imported to MATLAB program to calculate the LHTC instantaneously by the measurement of the heat flux per unit area maintained by the heat flux sensor and the temperature difference between the surface temperature and the bulk temperature, as shown in the following relation:

$$h_i = \frac{q_i}{(T_s - T_{bav})} \quad (1)$$

Where h_i is the instantaneous local heat transfer coefficient (W/m^2. °C), q_i is the instantaneous heat flux per unit area (W/m^2), T_{si} is the surface temperature measured instantaneously, and T_{bavg} is the average bulk temperature obtained from three thermocouples signals.

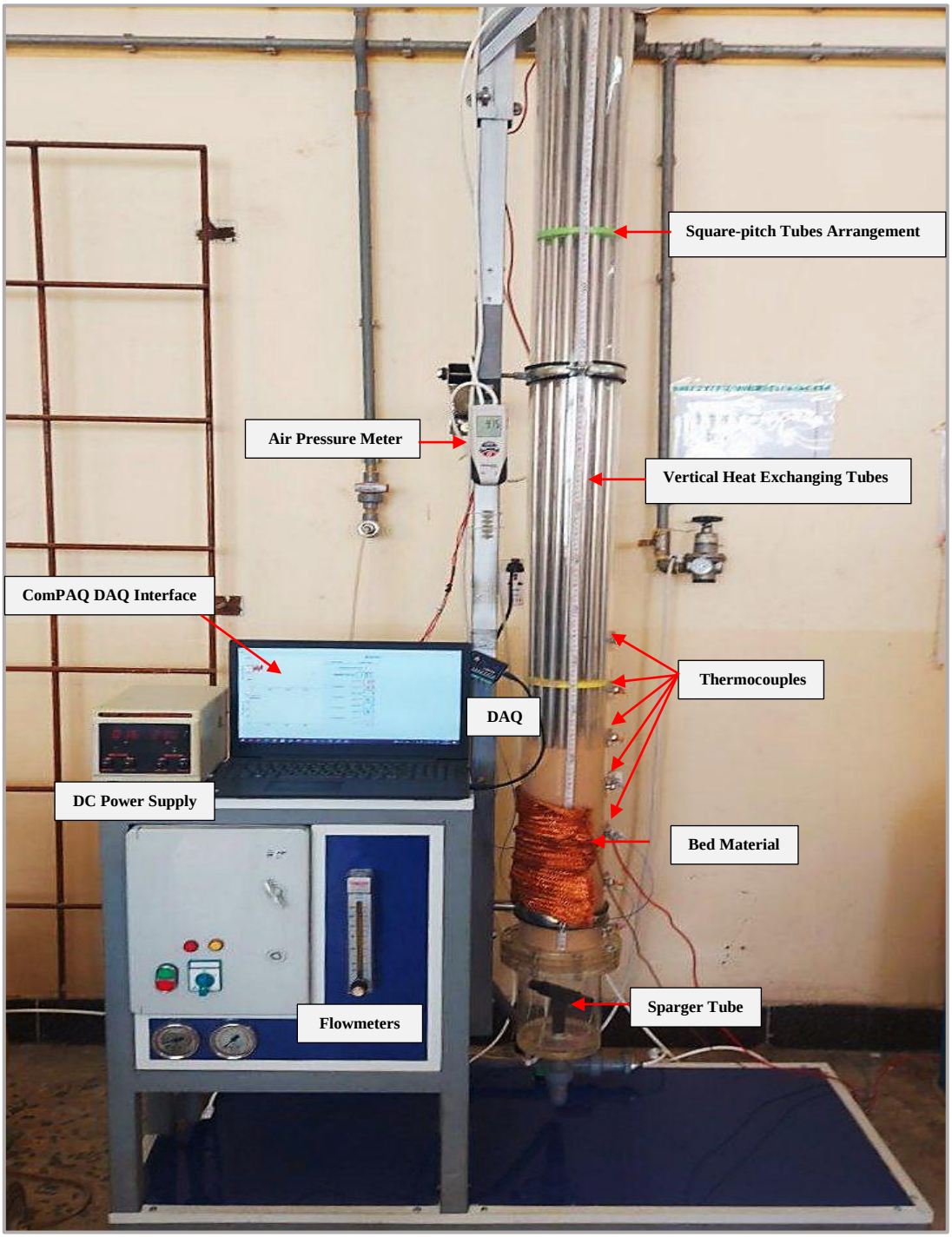

Figure 2: A photo of a fluidized bed reactor with vertical heat exchanging tubes

Furthermore, the local heat transfer coefficient measurements were accomplished within a wide range of superficial gas velocities at one axial height of 15 cm from the distributor plate and at four radial positions in the center of a square tube arrangement, as shown in Figure 3.

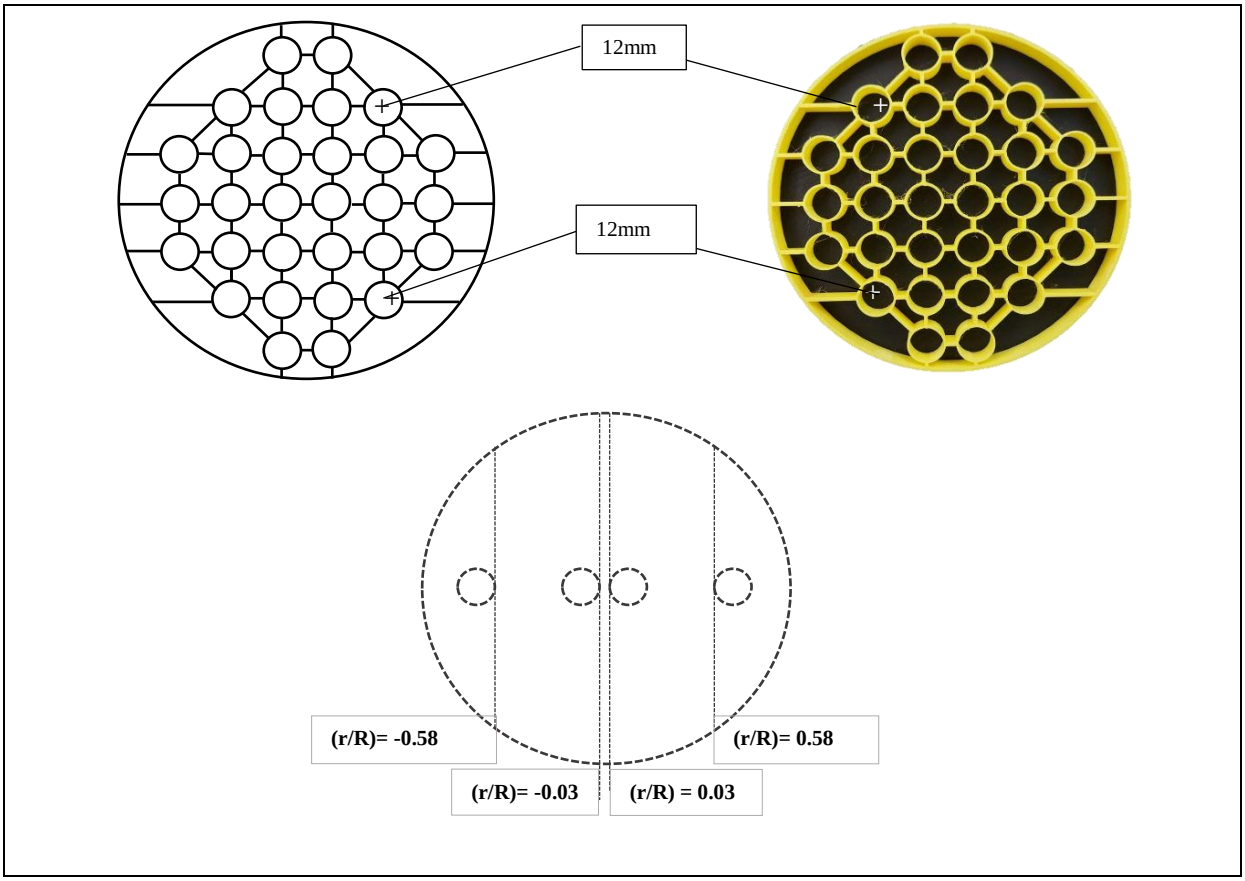

Figure 3: Schematic diagram and a photo of the designed square configuration with the radial positions of the measurements for stainless steel heat transfer probe along the column with vertical heat exchanging tubes

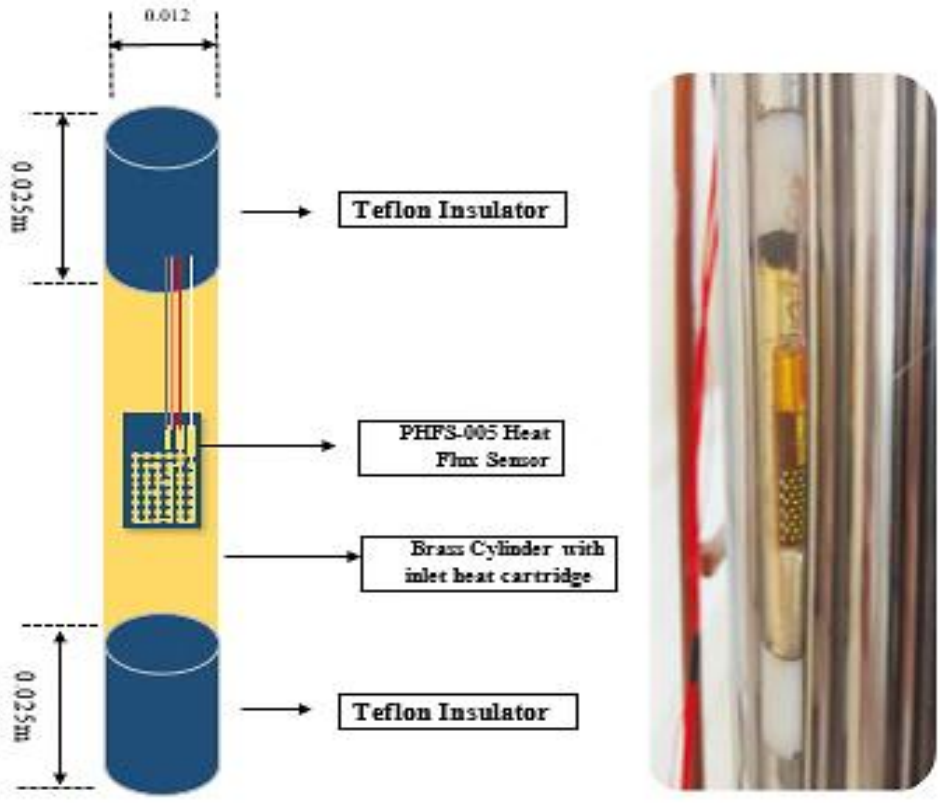

Figure 4: A photo and a schematic diagram for an advanced heat transfer probe

2.2.3 The reproducibility of the measurements

To validate the reproducibility of the advanced heat transfer technique, the measurements of the LHTC were replicated twice for two consecutive days for each superficial gas velocity. It is important to mention that each value of the LHTC was replicated at each velocity three times to reduce the experimental errors in the measurements. Therefore, only the average values of the heat transfer coefficient were presented in the results. As displayed in Figure 5, the replication of these measurements indicates that there is no need to replicate the measurements again at each condition since the percentage of relative differences for two days near the radial wall position of the square tube arrangement is 0.575 %.

Table 2: The specifications of PHFS heat flux sensor

Item	Details
Sensor Type	Differential-Temperature Thermopile
Nominal Sensitivity	Approx. 2.5mV/(W/cm^2)
Sensor Thickness(t)	Approx. 305 microns
Specific Thermal Resistivity	Approx. 0.9 K/(Kw/m^2)
Heat Flux Range	+/- 150 kW/m^2
Temperature Range	-50 °C to 120 °C
Sensor Surface Thermocouple	Type T
Sensing Area Dimensions	a=1.27 cm b=1.27cm
Total Sensor Dimensions	W=1.4 cm H=2.35 cm
Sensing Area (cm^2)	1.6 cm^2
Total Sensor Area (cm^2)	3.3 cm^2

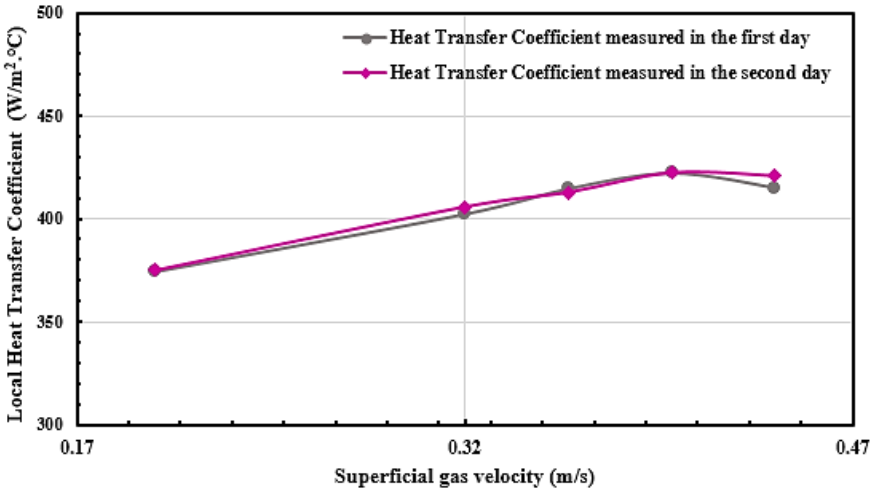

Figure 5: The reproducibility of the advanced heat transfer technique measurements at r/R = 0.58 near the wall at different superficial gas velocities

3. Results and Discussion

The local heat transfer coefficient was experimentally measured using an advanced heat transfer technique at four radial positions (r/R =+/- 0.58, +/- 0.03) with a wide range of superficial gas velocities (0.2-0.48) m/s. These four radial positions were chosen based on the presence of the internals from the wall region to the central region along the diameter of the column. The following sections represent the impact of superficial gas velocity and radial positions on the heat transfer locally and instantaneously at one axial position of (H/D =1.923) within the column.

3.1 The Impact of Superficial Gas Velocity on Local Heat Transfer Coefficient

The impact of using various superficial gas velocities on the heat transfer coefficient at different radial positions is illustrated in Figure 6. This figure demonstrates that the local heat transfer coefficient values near the wall improved as the superficial gas velocities increased for all the radial and axial positions. For example, when the superficial gas velocity increased from 0.2 m/s to 0.4 m/s, the local heat transfer coefficient was increased by 9.27%. On the other hand, different behavior was obtained near the center region. The local heat transfer coefficient still increases with the superficial gas velocity. Still, to a certain point from 0.2 m/s to 0.28 m/s, then it stabilize [34–36]. The difference between these two regions in the local heat transfer coefficient can be explained by the movement and the distribution of the

particles within the bed and the resistance of the particles in the presence of the vertical heat exchanging tubes with a square-pitch tube arrangement inside the reactor. As can be noticed from Figure 6b, in the center region (0.03), the local heat transfer coefficient increased suddenly with the superficial gas velocity from 0.2 m/s to 0.24 m/s by 37.4%, whereas, in Fig6d, the local heat transfer coefficient increased near the center region (-0.03) from 0.2 m/s to 0.28 by 54.2%, then it stabilized. This could eventually cause by the particle velocity increases in the case of vertical heat exchanging tubes with the superficial gas velocity within the column [34,36,37]. It was found that the local heat transfer coefficients were improved in the case of the vertical immersed tubes near the wall region (+/- 0.58) at higher superficial gas velocities and more uniformity than those near the center region.

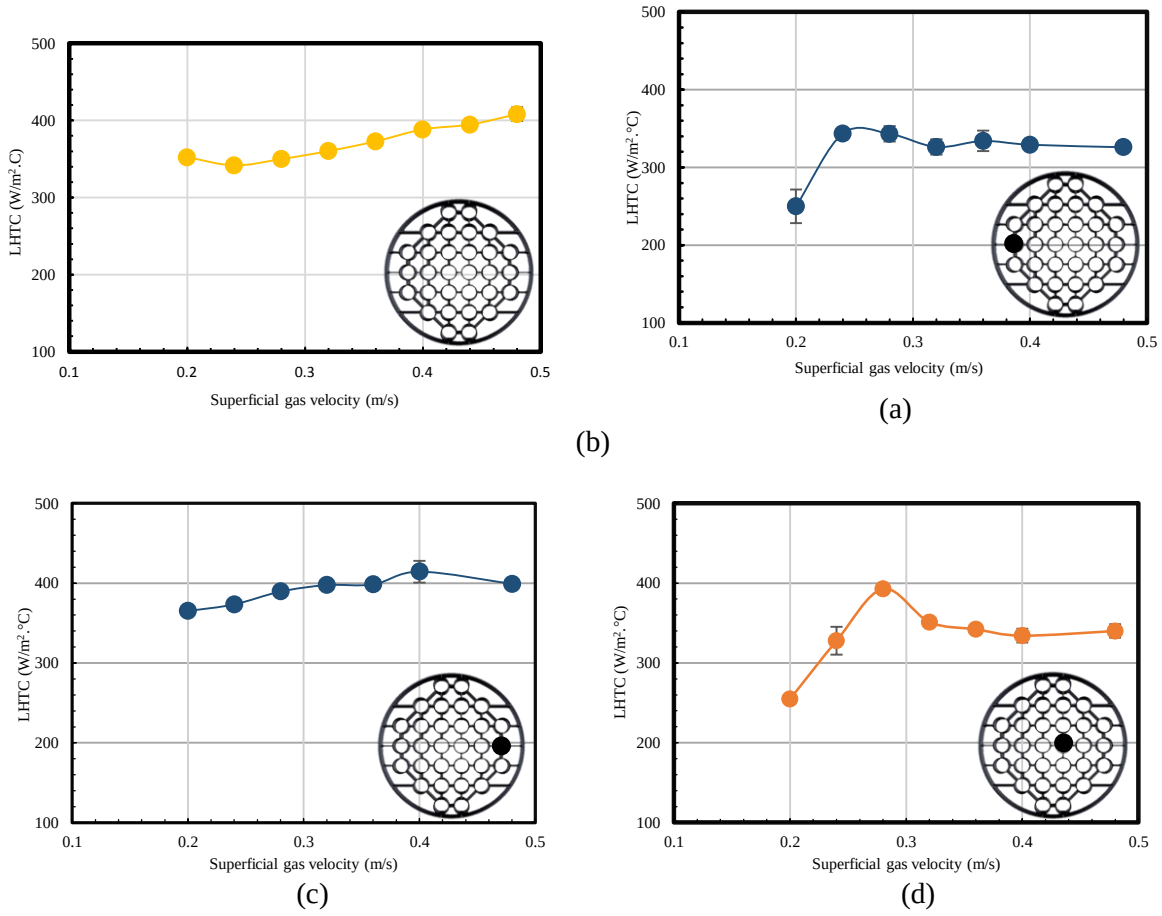

Figure 6: The effect of superficial gas velocity on the local heat transfer coefficient at different radial positions at H/D of 1.15 a) r/R = 0.58, b) r/R = 0.03, c) r/R = -0.58, d) r/R = -0.03

3.2 The Influence of Radial Positions on The Local Heat Transfer Coefficient

As presented in Figure 7, the local heat transfer coefficient increased near the wall region while decreasing in the core of the column with a wide range of superficial gas velocities. For example, the local heat transfer coefficient improved with the increase of superficial gas velocity depending on the radial profiles (r/R). As superficial gas velocity rose, maximum heat transfer coefficients were obtained at each radial position. Thus heat transfer coefficients with radial profiles were almost uniform [20, 37–39].

The heat transfer coefficients in the wall region were significantly higher than those in the center region by 28.9% as the superficial gas velocity increased. The differences remain minimal at low superficial gas velocities, but the variations become significant at high superficial gas velocities. This refers to the fact that bubbles with small diameters are uniformly distributed over the entire column area at low superficial gas velocities. Conversely, large bubbles establish as the superficial gas velocity rise, and many rises through the wall region of the column. Since the more free area to flow is provided by this arrangement near the wall region as compared with the center region [20,43,44].

Another important piece of evidence in enhancing the heat transfer is the flow behavior within the column, which can explain the variation of trends between the two regions during the turbulent fluidization regime. The center region along the column diameter suddenly changes from a flow behavior influenced by large, fast-moving particles. In contrast, the region along the walls tends to change from a dense layer of downward-moving gas and particle combination. As the velocity increases, both regions gradually transform into a structure dominated by rapidly moving particles suspended in a flow of aggressively mixing turbulent particles throughout the column [36,38,45–47].

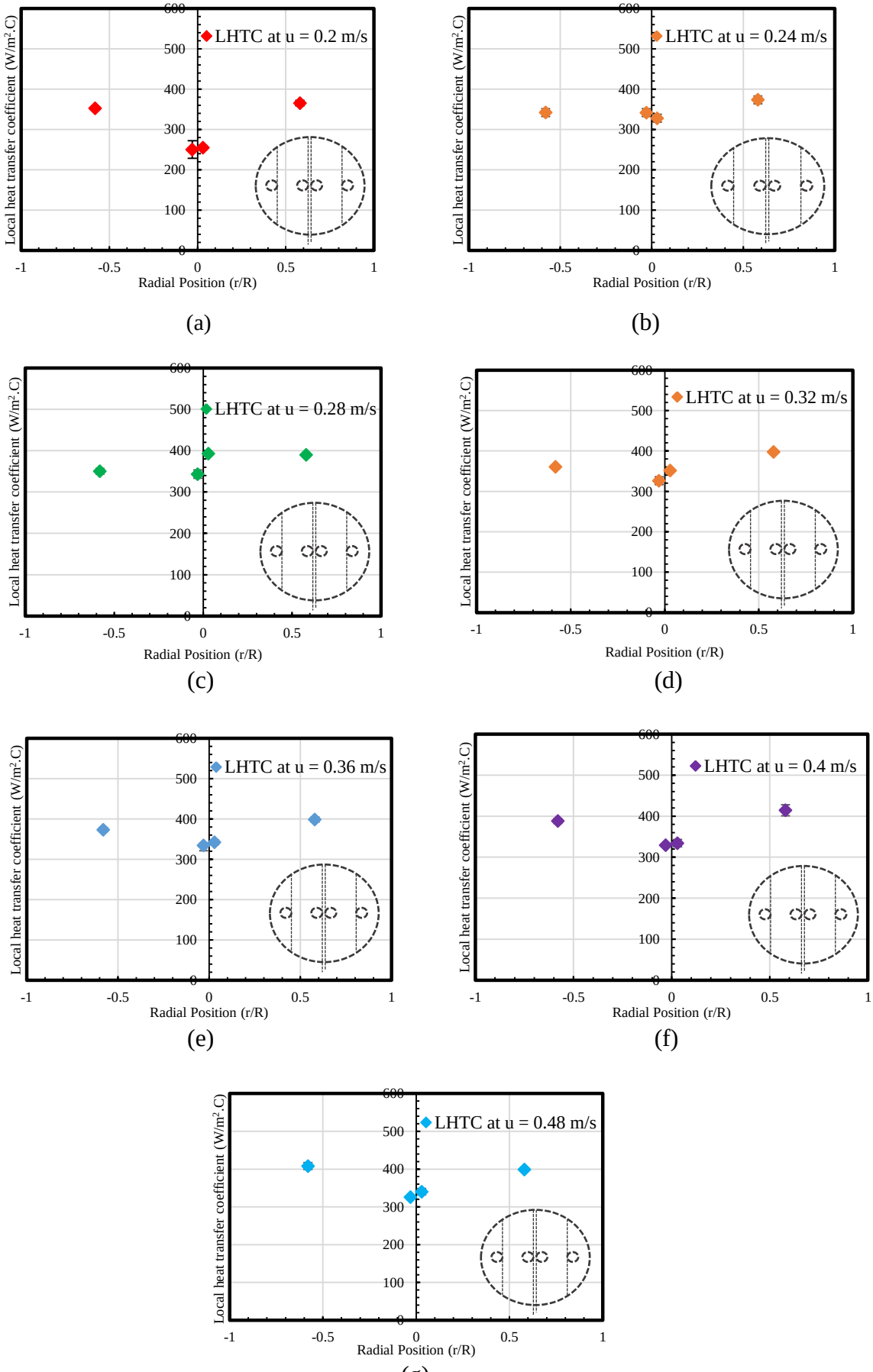

Figure 7: Heat transfer coefficient at different radial positions at H/D of 1.15: a) u=0.2m/s, b) u = 0.24m/s, c) u = 0.28m/s, d) u = 0.32m/s, e) u = 0.36m/s, f) u = 0.4m/s, g) u = 0.48m/s

3.3 Comparison of Heat Transfer Coefficient with Literature

The obtained results from this study for the heat transfer coefficient were compared with the previous studies of and Yasser [27] in gas-solid fluidized bed reactors without heat exchanging tubes and with the work of Al-Dahhan in the case of vertical heat exchanging tubes with circular tube arrangement for Glass Beads particles [48]. The comparison for heat transfer coefficient was carried out at a radial position near the center region (0.03) with a wide range of superficial gas velocities (0.2-0.3) m/s.

As shown in Figure 8, higher local heat transfer coefficient values were obtained in the experimental results for vertical heat exchanging tubes with square-pitch tube arrangement. The behavior of the local heat transfer coefficient increased with the superficial gas velocity to a certain point and then decreased until it stabilized. While, for the case without heat exchange tubes, the obtained experimental results for local heat transfer coefficient increase uniformly when the superficial gas velocity increases. Accordingly, the square tube arrangement offers a higher local heat transfer coefficient value than the circular tube arrangement. This will improve the heat transfer efficiency and the reactor performance in such types of multiphase reactors [39–42].

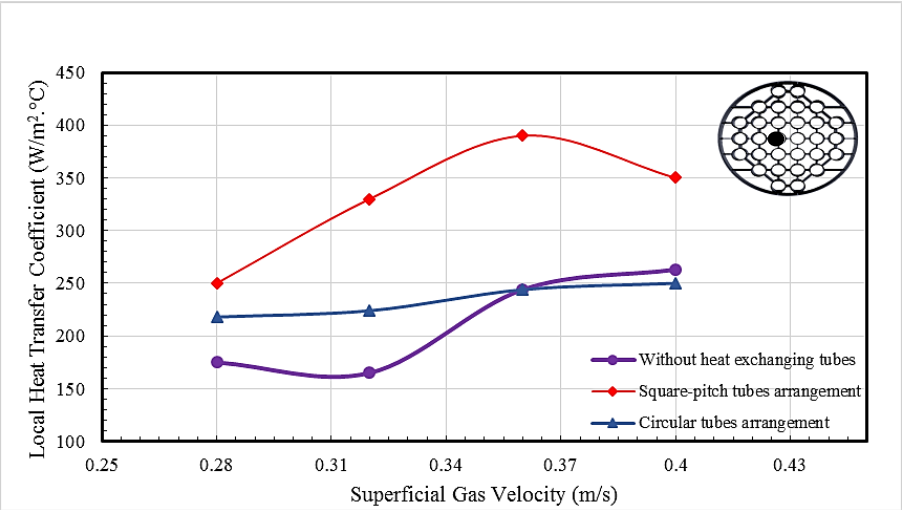

Figure 8: A comparison of the heat transfer coefficient with literature at different superficial gas velocities

4. Conclusion

Based on the extensive research results obtained in this experimental study, several remarks can be made:

1) A new experimental data acquisition instrument has been implemented to quantify the impact of vertical heat exchanging tubes on heat transfer by measuring the local heat transfer coefficient instantaneously with the heat transfer probe technique.
2) Experimental results have shown that the local heat transfer coefficient increased rapidly from the core region to the wall region regarding the particle distribution and the distance between the tubes with a wide range of superficial gas velocities.
3) Generally, the local heat transfer coefficient increases the superficial gas velocity for all radial and axial positions.
4) The presented results also investigated that the local heat transfer coefficient in a fluidized bed reactor equipped with a bundle of vertical tubes increases substantially as the superficial gas velocity increases at the wall region. In contrast, a different behavior was realized at the reactor's core.

Acknowledgment

The authors would like to acknowledge the chemical engineering department, University of Technology- Iraq, for their guidance and support throughout this study.

Author contribution

All authors contributed equally to this work.

Funding

This research received no external funding

Data availability statement

The data that support the findings of this study are available on request from the corresponding author.

Conflicts of interest

Authors declare that their present work has no conflict of interest with other published works.

References

[1] J. Karl and T. Pröll, Steam gasification of biomass in dual fluidized bed gasifiers: A review, *Renew. Sustain. Energy Rev.*, 98 (2018) 64–78, doi: 10.1016/j.rser.2018.09.010.

[2] M. Shahabuddin, M. T. Alam, B. B. Krishna, T. Bhaskar, and G. Perkins, A review on the production of renewable aviation fuels from the gasification of biomass and residual wastes, *Bioresour. Technol.*, 312 (2020) 123596, doi: 10.1016/j.biortech.2020.123596.

[3] G. Zang, P. Sun, A. A. Elgowainy, A. Bafana, and M. Wang, Performance and cost analysis of liquid fuel production from H2and CO2based on the Fischer-Tropsch process, *J. CO2 Util.*, 46 (2021) 101459, doi: 10.1016/j.jcou.2021.101459.

[4] I. Hannula, N. Kaisalo, and P. Simell, Preparation of Synthesis Gas from CO2 for Fischer–Tropsch Synthesis—Comparison of Alternative Process Configurations,*C—Journal Carbon Res.*, 6 (2020) 55 doi: 10.3390/c6030055.

[5] R. G. dos Santos and A. C. Alencar, Biomass-derived syngas production via gasification process and its catalytic conversion into fuels by Fischer Tropsch synthesis: A review, *Int. J. Hydrogen Energy*, 45 (2020) 18114–18132. doi: 10.1016/j.ijhydene.2019.07.133.

[6] M. Kagumba, H. Al-Naseri, and M. H. Al-Dahhan, A new contact time model for the mechanistic assessment of local heat transfer coefficients in bubble column using both the four-optical fiber probe and the fast heat transfer probe-simultaneously,*Chem. Eng. J.*, 361 (2018) 67–79, 2019. doi: 10.1016/j.cej.2018.12.046.

[7] M. Pasha, G. Li, M. Shang, S. Liu, and Y. Su, Mass transfer and kinetic characteristics for CO2 absorption in microstructured reactors using an aqueous mixed amine, *Sep. Purif. Technol.*, 274 (2021) 118987, 2021. doi: 10.1016/j.seppur.2021.118987.

[8] S. I. Ngo, Y. Il Lim, D. Lee, and M. W. Seo, Flow behavior and heat transfer in bubbling fluidized-bed with immersed heat exchange tubes for CO2 methanation, *Powder Technol.*, 380 (2021) 462–474, 2021, doi: 10.1016/j.powtec.2020.11.027.

[9] X. Guan, Q. Xu, N. Yang, and K. D. P. Nigam, Hydrodynamics in Bubble Columns with Helically-Finned Tube Internals: Experiments and CFD-PBM Simulation, *Chem. Eng. Sci.*, (2021) 116674, doi: 10.1016/j.ces.2021.116674.

[10] Y. Cochet, C. Briens, F. Berruti, J. McMillan, and F. J. Sanchez Careaga, Impact of column geometry and internals on gas and particle flows in a fluidized bed with downward solids circulation: Effect of lateral injection profile and baffles, *Powder Technol.*, 372 (2021) 275–289, 2020, doi: 10.1016/j.powtec.2020.05.071.

[11] W. J. Huang, C. T. Yu, W. J. Sheu, and Y. C. Chen, The effect of non-uniform temperature on the sorption-enhanced steam methane reforming in a tubular fixed-bed reactor,*Int. J. Hydrogen Energy*, 46 (2021) 16522–16533, 2021, doi: 10.1016/j.ijhydene.2020.07.182.

[12] A. A. Jasim, A. J. Sultan, and M. H. Al-Dahhan, Influence of heat-exchanging tubes diameter on the gas holdup and bubble dynamics in a bubble column, *Fuel*, 236 (2019) 63–82,2019, doi: 10.1016/j.ijmultiphaseflow.2018.11.008.

[13] V. Verma, T. Li, J. Dietiker, and W. A. Rogers, Sub-grid drag model for immersed vertical cylinders in fl uidized beds, *Powder Technol.*, 2017, doi: 10.1016/j.powtec.2016.12.044.

[14] X. Zhang, W. Qian, H. Zhang, Q. Sun, and W. Ying, Effect of the operation parameters on the Fischer–Tropsch synthesis in fluidized bed reactors, *Chinese J. Chem. Eng.*, 26 (2018) 245–251, 2018, doi: 10.1016/j.cjche.2017.05.012.

[15] H. Taofeeq and M. Al-Dahhan, The impact of vertical internals array on the key hydrodynamic parameters in a gas-solid fluidized bed using an advance optical fiber probe, *Adv. Powder Technol.*, 29 (2018) 2548–2567. doi: 10.1016/j.apt.2018.07.008.

[16] B. Lv, X. Deng, Z. Luo, Y. Fu, C. Chen, and X. Xu, Impact of vertical internals on the hydrodynamics and separation performance of a gas–solid separation fluidized bed, *Powder Technol.*, 360 (2020) 577–587. doi: 10.1016/j.powtec.2019.10.071.

[17] N. Nemati, P. Andersson, V. Stenberg, and M. Rydén, Experimental Investigation of the Effect of Random Packings on Heat Transfer and Particle Segregation in Packed-Fluidized Bed, *Ind. Eng. Chem. Res.*, 60 (2021) 10365–10375. doi: 10.1021/acs.iecr.1c01221.

[18] L. von Berg, A. Soria-Verdugo, C. Hochenauer, R. Scharler, and A. Anca-Couce, Evaluation of heat transfer models at various fluidization velocities for biomass pyrolysis conducted in a bubbling fluidized bed, *Int. J. Heat Mass Transf.*, 160, (2020) 120175, 2020, doi: 10.1016/j.ijheatmasstransfer.2020.120175.

[19] A. J. Sultan, L. S. Sabri, and M. H. Al-Dahhan, Impact of heat-exchanging tube configurations on the gas holdup distribution in bubble columns using gamma-ray computed tomography, *Int. J. Multiph. Flow*, 106 (2018) 202–219, doi: 10.1016/j.ijmultiphaseflow.2018.05.006.

[20] A. J. Sultan, L. S. Sabri, and M. H. Al-Dahhan, Investigating the influence of the configuration of the bundle of heat exchanging tubes and column size on the gas holdup distributions in bubble columns via gamma-ray computed tomography, *Exp. Therm. Fluid Sci.*, 2018, doi: 10.1016/j.expthermflusci.2018.05.005.

[21] F. Schillinger, S. Maurer, E. C. Wagner, J. R. Van Ommen, R. F. Mudde, and T. J. Schildhauer, PT US CR, *Int. J. Multiph. Flow*, 2017, doi: 10.1016/j.ijmultiphaseflow.2017.07.013.

[22] C. Vargas-salgado, E. Hurtado-pérez, D. Alfonso-solar, and A. Malmquist, Empirical design, construction, and experimental test of a small-scale bubbling fluidized bed reactor, *Sustain.*, 13(2021) 1–23, 2021. doi: 10.3390/su13031061.

[23] J. Chladek, C. K. Jayarathna, B. M. E. Moldestad, and L. A. Tokheim, Fluidized bed classification of particles of different size and density, *Chem. Eng. Sci.*, 177 (2018) 151–162. doi: 10.1016/j.ces.2017.11.042.

[24] J. M. Ali, A. J. Sultan, and B. J. Kadhim, Experimental investigation and COMSOL modeling for different geometrical configurations of extended surfaces, *Heat Transf.*, 50 (2021) 1612–1630, doi: 10.1002/htj.21944.

[25] M. Hamzehei, Study of Heat Transfer and Hydrodynamics in the Fluidized Bed Reactors, *Heat Transf. - Math. Model. Numer. Methods Inf. Technol.*, 2011, doi: 10.5772/14565.

[26] A. Stefanova, H. T. Bi, J. C. Lim, and J. R. Grace, Local hydrodynamics and heat transfer in fluidized beds of different diameter, *Powder Technol.*, 212 (2011) 57–63, 2011, doi: 10.1016/j.powtec.2011.04.026.

[27] M. A. Shrshab and Y. I. Abdulaziz, Determination of Heat Transfer Coefficients in Air-Solid Fluidized Bed, *IOP Conf. Ser. Mater. Sci. Eng.*, 928, (2020), doi: 10.1088/1757-899X/928/2/022067.

[28] V. Stenberg, V. Sköldberg, L. Öhrby, and M. Rydén, Evaluation of bed-to-tube surface heat transfer coefficient for a horizontal tube in bubbling fluidized bed at high temperature, *Powder Technol.*,352 (2019) 488–500, doi: 10.1016/j.powtec.2019.04.073.

[29] N. Masoumifard, N. Mostoufi, and R. Sotudeh-Gharebagh, Prediction of the maximum heat transfer coefficient between a horizontal tube and gas-solid fluidized beds, *Heat Transf. Eng.*, 31 (2010) 870–879, doi: 10.1080/01457630903550275.

[30] N. S. Grewal and S. C. Saxena, Heat transfer between a horizontal tube and a gas-solid fluidized bed, *Int. J. Heat Mass Transf.*, 23 (1980) 1505–1519, 1980, doi: 10.1016/0017-9310(80)90154-4.

[31] X. Wu, Y. Li, X. Zhu, L. Huang, and X. Zhu, Experimental study on fluidization behaviors of walnut shell in a fluidized bed assisted by sand particles, *RSC Adv.*, 8 (2018) 40279–40287, doi: 10.1039/C8RA07959E.

[32] M. A. Izquierdo-Barrientos, M. Fernández-Torrijos, J. A. Almendros-Ibáñez, and C. Sobrino, Experimental study of fixed and fluidized beds of PCM with an internal heat exchanger, *Appl. Therm. Eng.*, 106 (2016) 1042–1051. doi: 10.1016/j.applthermaleng.2016.06.049.

[33] A. A. Jasim, A. J. Sultan, and M. H. Al-Dahhan, Impact of heat exchanging internals configurations on the gas holdup and bubble properties in a bubble column, *Int. J. Multiph. Flow*, 112 (2019) 63–82. doi: 10.1016/j.ijmultiphaseflow.2018.11.008.

[34] A. A. Youssef and M. H. Al-Dahhan, Impact of internals on the gas holdup and bubble properties of a bubble column, *Ind. Eng. Chem. Res.*, 48 (2009) 8007–8013. doi: 10.1021/ie900266q.

[35] U. Kumar and V. K. Agarwal, Biomass gasification in a fluidized bed reactor: Hydrodynamics and heat transfer studies, *Numer. Heat Transf. Part A Appl.*, 70 (2016) 513–531. doi: 10.1080/10407782.2016.1177340.

[36] P. Li, R. Hou, C. Zhang, and T. Wang, Hydrodynamic behaviors of a spouted fluidized bed with a conical distributor and auxiliary inlets for the production of polysilicon with wide-size-distribution particles,*Chem. Eng. Sci.*, 247 (2022) 117069. doi: 10.1016/j.ces.2021.117069.

[37] A. Efhaima and M. H. Al- Dahhan, Validation of the new mechanistic scale-up of gas-solid fluidized beds using advanced non-invasive measurement techniques, *Can. J. Chem. Eng.*, 2021, 2020. doi: 10.1002/cjce.23938.

[38] H. J. Das, P. Mahanta, and R. Saikia, Characterization of sand particles in a bubbling fluidized bed with diverging riser, *Int. Commun. Heat Mass Transf.*, 119 (2021) 104953. doi: 10.1016/j.icheatmasstransfer.2020.104953.

[39] S. Ge *et al.*, Electrostatic effects on hydrodynamics in the riser of the circulating fluidized bed for polypropylene, *AIChE J.*, 66 (2020) 1–13, 2020, doi: 10.1002/aic.16916.

[40] R. S. Abdulmohsin, B. A. Abid, and M. H. Al-dahhan, Chemical Engineering Research and Design Heat transfer study in a pilot-plant scale bubble column,*Chem. Eng. Res. Des.*, 89 (2021) 78–84, doi: 10.1016/j.cherd.2010.04.019.

[41] A. K. Jhawar and A. Prakash, Influence of bubble column diameter on local heat transfer and related hydrodynamics, *Chem. Eng. Res. Des.*, 89 (2011) 1996–2002. doi: 10.1016/j.cherd.2010.11.019.

[42] A. Yadav and S. Roy, Void fraction distribution for convective boiling flows in single and multiple heater rods assembly, *Chem. Eng. Sci.*, 247 (2022) 117063. doi: 10.1016/j.ces.2021.117063.

[43] X. Guan and N. Yang, Characterizing regime transitions in a bubble column with internals, *AIChE J.*, 67 (2021)1–15. doi: 10.1002/aic.17167.

[44] A. A. Youssef, M. E. Hamed, J. T. Grimes, M. H. Al-Dahhan, and M. P. Duduković, Hydrodynamics of pilot-scale bubble columns: Effect of internals, *Ind. Eng. Chem. Res.*, 2013, doi: 10.1021/ie300465t.

[45] P. C. Bisognin, J. M. Fusco, and C. Soares, Heat transfer in fluidized beds with immersed surface: Effect of geometric parameters of surface, *Powder Technol.*, 297 (2016) 401–408, doi: 10.1016/j.powtec.2016.04.028.

[46] C. G. Philippsen, A. C. F. Vilela, and L. D. Zen, Fluidized bed modeling applied to the analysis of processes: Review and state of the art, *J. Mater. Res. Technol.*, 4 (2015) 208–216, doi: 10.1016/j.jmrt.2014.10.018.

[47] L. Wang *et al.*, Experimental and numerical investigation of particle flow and mixing characteristics in an internally circulating fluidized bed, *J. Chem. Eng. Japan*, 52 (2019) 89–98, doi: 10.1252/jcej.18we014.

[48] H. Taofeeq and M. Al-Dahhan, Heat transfer and hydrodynamics in a gas-solid fluidized bed with vertical immersed internals, *Int. J. Heat Mass Transf.*, 122 (2018) 229–251, doi: 10.1016/j.ijheatmasstransfer.2018.01.093.